Molecular Therapy
Oncolytics
Original Article

Vaccinia virus and peptide-receptor radiotherapy synergize to improve treatment of peritoneal carcinomatosis

Kathryn Ottolino-Perry,[1,2] David Mealiea,[1,2,6] Clara Sellers,[1] Sergio A. Acuna,[1] Fernando A. Angarita,[1,2] Lili Okamoto,[2,6] Deborah Scollard,[3] Mihaela Ginj,[2] Raymond Reilly,[4] and J. Andrea McCart[1,2,5,6]

[1]Toronto General Research Institute, University Health Network, 200 Elizabeth Street, M5G 2C4 Toronto, ON, Canada; [2]Institute of Medical Science, University of Toronto, 1 King's College Circle, M5S 1A8 Toronto, ON, Canada; [3]STTARR, Radiation Medicine Program, Princess Margaret Hospital, UHN, 610 University Avenue, M5G 2C1 Toronto, ON, Canada; [4]Leslie Dan Faculty of Pharmacy, University of Toronto, 144 College Street, M5S 3M2 Toronto, ON, Canada; [5]Department of Surgery, Mount Sinai Hospital and University of Toronto, 600 University Avenue, M5G 1X5 Toronto, ON, Canada

Tumor-specific overexpression of receptors enables a variety of targeted cancer therapies, exemplified by peptide-receptor radiotherapy (PRRT) for somatostatin receptor (SSTR)-positive neuroendocrine tumors. While effective, PRRT is restricted to tumors with SSTR overexpression. To overcome this limitation, we propose using oncolytic vaccinia virus (vvDD)-mediated receptor gene transfer to permit molecular imaging and PRRT in tumors without endogenous SSTR overexpression, a strategy termed radiovirotherapy. We hypothesized that vvDD-SSTR combined with a radiolabeled somatostatin analog could be deployed as radiovirotherapy in a colorectal cancer peritoneal carcinomatosis model, producing tumor-specific radiopeptide accumulation. Following vvDD-SSTR and ^{177}Lu-DOTATOC treatment, viral replication and cytotoxicity, as well as biodistribution, tumor uptake, and survival, were evaluated. Radiovirotherapy did not alter virus replication or biodistribution, but synergistically improved vvDD-SSTR-induced cell killing in a receptor-dependent manner and significantly increased the tumor-specific accumulation and tumor-to-blood ratio of ^{177}Lu-DOTATOC, making tumors imageable by microSPECT/CT and causing no significant toxicity. ^{177}Lu-DOTATOC significantly improved survival over virus alone when combined with vvDD-SSTR but not control virus. We have therefore demonstrated that vvDD-SSTR can convert receptor-negative tumors into receptor-positive tumors and facilitate molecular imaging and PRRT using radiolabeled somatostatin analogs. Radiovirotherapy represents a promising treatment strategy with potential applications in a wide range of cancers.

INTRODUCTION

Tumor-specific overexpression of cell-surface receptors is the foundation upon which many targeted cancer therapies, such as peptide-receptor radiotherapy (PRRT), have been developed. PRRT, which involves the systemic delivery of radiolabeled peptides, is most frequently used in patients with somatostatin receptor (SSTR)-positive neuroendocrine tumors (NETs).[1,2] The development of reliable radiolabeling methods that can stably link one of the many available somatostatin (SS) analogs (e.g., pentetreotide, octreotide, octreotate, etc.) with one of a selection of radionuclides (e.g., ^{177}Lu, ^{90}Y, ^{111}In, and ^{68}Ga) using a metal chelator such as 1,4,7,10-tetraazacyclododecane-N,N′,N″,N‴-tetraacetic acid (DOTA) has led to the use of these radiopeptides (RPs) as both diagnostic and therapeutic agents. In patients with NETs, pretreatment molecular imaging is used to identify SSTR-positive primary and metastatic tumors, and sophisticated software can quantify the uptake in individual tissue compartments, thereby permitting patient-specific dosimetric calculations that predict the toxicity to normal tissues as a result of PRRT.

This targeted treatment approach is particularly beneficial for patients with metastatic disease that is inoperable,[3,4] as evidenced by the significant survival benefit in NET patients following the clinical introduction of PRRT.[5] Given the success of PRRT in this patient population, its investigational use has been extended to patients with other advanced and metastatic cancers[6,7]; however, it remains limited to use in those with tumor-specific SSTR overexpression. To overcome this limitation, oncolytic virus (OV)-mediated receptor gene transfer has been investigated as a tool to permit molecular imaging and targeted radiotherapy using radiopharmaceuticals that specifically bind to these receptors in tumors that do not have endogenous receptor overexpression. This multimodality treatment strategy, termed radiovirotherapy,[8] has been studied using a variety of OVs (e.g., vaccinia virus, measles virus, herpesvirus, and adenovirus) and receptor/ligand pairs,[9] including SSTR with radiolabeled SS analogs[10,11] and, more frequently, human sodium iodide symporter (NIS) with radioactive

Received 2 March 2021; accepted 5 April 2023;
https://doi.org/10.1016/j.omto.2023.04.001.

[6]Present address: Lunenfeld-Tanenbaum Research Institute, Mount Sinai Hospital, Toronto, ON Canada

Correspondence: Dave Mealiea, Room 1225, Mount Sinai Hospital, 600 University Avenue, Toronto, ON M5G 1X5, Canada.
E-mail: d.mealiea@mail.utoronto.ca

iodide (e.g., ^{131}I).[12–19] This approach, which allows radioligand targeting of tumors with low endogenous receptor expression through virus-mediated receptor gene delivery, has diagnostic and therapeutic applications with the potential for synergistic enhancement of treatment efficacy by taking advantage of the oncolytic effects of viruses and the DNA-damaging effects of radiation.[19,20]

Early studies designed to improve and expand the applicability of PRRT utilized a gene therapy approach involving non-replicating viruses as the receptor-delivery vector.[21] In these studies, radiation was the sole therapeutic agent and tumor cell death was dependent on delivery of the radiation dose to both the transduced cell (to which the radioligand bound) and the uninfected neighboring cells. Transduction efficiency was a major limitation of these studies, as non-replicating viruses demonstrated very minimal spread,[22] leading to similarly limited and heterogeneous radioligand accumulation throughout the tumor volume.[23] Radiovirotherapy relies on the tumor killing capacity of both the virus and the radioligand. OVs are highly cytolytic replicating viruses; therefore, it is generally assumed that infected tumor cells will die as a result of viral infection. The benefit of the radioligand exists in the ability to deliver a radiation dose to uninfected neighboring cells through the radiation crossfire effect, first demonstrated by Dingli and colleagues.[24]

Vaccinia virus (VV) is a potent oncolytic vector capable of high levels of tumor-specific replication and transgene expression.[25] Oncolytic VV has demonstrated excellent anti-tumor efficacy in numerous preclinical models[26] and is currently being investigated in clinical trials, with promising results.[27–33] We have previously demonstrated that an attenuated oncolytic VV with deletions in two viral genes (vaccinia growth factor and viral thymidine kinase) and encoding the human SSTR subtype 2A (vvDD-SSTR) results in specific accumulation of an ^{111}In-labeled SS analog in a subcutaneous colorectal cancer (CRC) tumor model.[10] While this study demonstrated the *in vivo* RP-accumulating activity of vvDD-SSTR, it did not evaluate the therapeutic effect of combination therapy. Improved cell killing over virus alone was later demonstrated in an *in vitro* CRC tumor spheroid model using ^{111}In- and ^{177}Lu-DOTA-octreotide (DOTATOC).

To date, most radiovirotherapy studies have utilized subcutaneous tumor models[14,17,19,34–37] with only a minority investigating efficacy in disseminated tumor models, which more closely resemble the type of disease (i.e., unresectable) most likely to benefit from PRRT.[38–41] The objective of this study was to evaluate the therapeutic efficacy of SSTR-mediated radiovirotherapy using vvDD-SSTR in a disseminated CRC tumor model. vvDD has previously been reported to improve survival in disseminated ovarian,[42] mesothelioma,[43] and CRC carcinomatosis models,[44] and we have recently demonstrated that vvDD-SSTR increases the median survival in both syngeneic and xenograft models of CRC carcinomatosis.[45,46] We hypothesize that vvDD-SSTR will enable the imaging and improved treatment of intraperitoneal CRC tumors using ^{177}Lu-DOTATOC due to virus-directed tumor-specific accumulation of the RPs.

RESULTS

vvDD-SSTR and ^{177}Lu-DOTATOC synergistically increase cytotoxicity toward CRC cells

DLD1 human CRC cells were treated with vvDD-SSTR and/or ^{177}Lu-DOTATOC (37–740 kBq/well; 1.2 ng per 37 kBq) and assayed for virus replication and cell viability (Figure 1). ^{177}Lu-DOTATOC had no effect on virus replication at all radioactivities tested (Figure 1A). The effect of combination therapy on cell viability was evaluated in cells infected with vvDD-SSTR (MOI 0.01–5) (Figures 1B and 1C) or a receptor-negative control virus, vvDD-red fluorescent protein (RFP) (MOI 0.1–1) (Figure 1D). When given alone, both vvDD-SSTR (Figures 1B) and ^{177}Lu-DOTATOC (Figure 1C) had a dose-response effect. ^{177}Lu-DOTATOC did not decrease cell viability at 37 kBq but showed significant cytotoxicity at 370 and 740 kBq in the absence of virus infection and therefore receptor expression. This indicates that, at these high doses, ^{177}Lu-DOTATOC-induced loss of cell viability is mainly receptor independent and a result of the non-specific irradiation of cells during the 4 h incubation period. At the 37 kBq dose of ^{177}Lu-DOTATOC, cell killing was significantly improved over either monotherapy when cells were infected at an MOI $\geq$1 (Figure 1C). This enhanced cell killing was receptor dependent, as the same dose of ^{177}Lu-DOTATOC did not affect cell viability in cells infected with a receptor-negative control virus (Figure 1D). An MOI of 5 was not used in this experiment because of its substantial cell killing effect independent of ^{177}Lu-DOTATOC, which would obscure the ability to evaluate the ^{177}Lu-DOTATOC effect. When cells were treated at lower MOIs (0.01 and 0.1) of vvDD-SSTR, addition of high-dose (370 and 740 kBq) ^{177}Lu-DOTATOC improved cell killing over virus alone, but not ^{177}Lu-DOTATOC alone, whereas addition of low-dose (37 kBq) ^{177}Lu-DOTATOC had no effect on cell viability relative to either monotherapy (Figures 1B and 1C). Taken together, these data suggest there is likely a threshold of receptor expression required to see a therapeutic benefit *in vitro* following combination therapy at doses of ^{177}Lu-DOTATOC.

Dose-response data (Figures 1B and 1C) were analyzed using the Chou-Talalay method for quantifying drug-drug interactions.[47] Synergy was observed at MOIs 1 and 5 when combined with 37 MBq, as well as at MOIs 0.01–1 when combined with 370 or 740 MBq of ^{177}Lu-DOTATOC (Figure 1C). The synergy observed at the higher doses of ^{177}Lu-DOTATOC was likely receptor expression independent, as there was minimal effect of virus at those highly cytotoxic doses (Figure 1B).

vvDD-SSTR results in expression of SSTR in intraperitoneal colorectal cancer tumors with low endogenous receptor expression

In vivo virus-directed expression of SSTR in peritoneally disseminated CRC tumors was confirmed by immunohistochemistry (IHC). DLD1 tumor-bearing mice were treated with 10^9 plaque-forming units (PFU) of vvDD-SSTR and sacrificed at 3, 5, 7, and 9 days post-infection (dpi). Multiple tumors per mouse were harvested and divided into two pieces for either IHC or titering. Staining

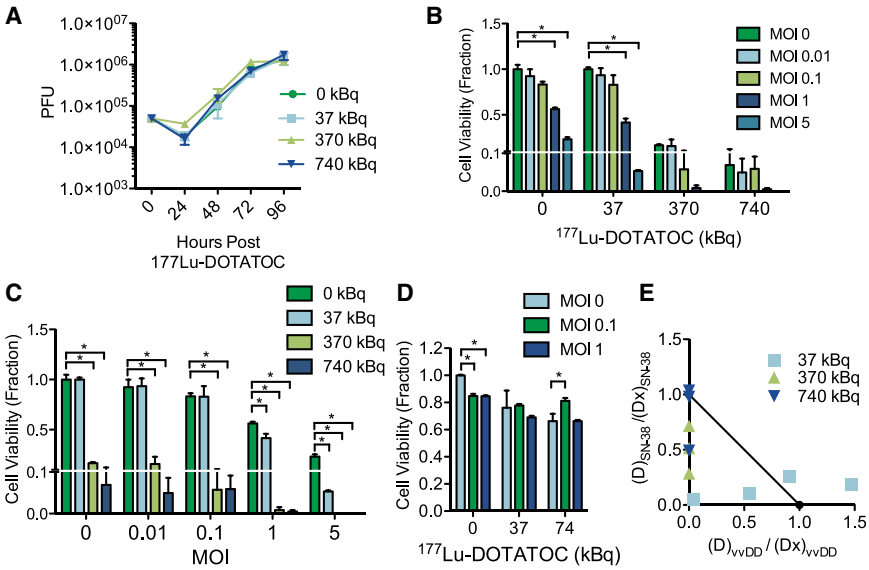

Figure 1. ^{177}Lu-DOTATOC synergistically improves vvDD-SSTR-induced cytotoxicity

DLD1 cells were infected with vvDD-SSTR for 24 h and incubated in the presence or absence of increasing activities of ^{177}Lu-DOTATOC (37–740 kBq; 1.2 ng per 37 kBq) for 4 h. (A) vvDD- SSTR (MOI 0.1) replication was determined up to 96 h post-^{177}Lu-DOTATOC treatment. (B–D) Cell viability was determined by MTS assay in cells infected with vvDD-SSTR (B and C; MOI 0.01–5) or vvDD-RFP, i.e., empty virus (D; MOI 0.1–1) at 72 h post-^{177}Lu-DOTATOC treatment. Data in (B) and (C) are from the same experiment. (E) Dose-response data (from B and C) were analyzed by the Chou-Talalay method for determining drug-drug interactions and plotted on a normalized isobologram. Data points falling below the solid line represent synergistic interactions. All bars represents the mean ± SEM. *p < 0.05, one-way ANOVA with Bonferroni's multiple-comparison test.

for VV and SSTR (subtype 2) on serial sections showed expression of SSTR in vvDD-SSTR-infected tumors but not in Hank's balanced salt solution (HBSS)-treated control tumors (Figure 2A). Quantification of staining expressed as the percentage positive pixels relative to total pixels showed that both VV and SSTR2 staining peaked on day 5 (Figures 2B and 2C), which was consistent with the tumor titers (Figure 2E). Staining for both VV and SSTR, as well as virus titers, declined by 9 dpi (data not shown). SSTR expression localized specifically to areas of VV staining within the tumors (Figure 2A), and there was a strong positive correlation between VV and SSTR staining among all the tumors harvested (Figure 2D).

Virus-mediated SSTR expression results in specific uptake of ^{177}Lu-DOTATOC in CRC tumors

Tumor-bearing mice were treated with 10^9 PFU of vvDD-SSTR or vvDD-enhanced green fluorescent protein (EGFP), a receptor-negative control virus, followed by 3.5 MBq (29.5–31 MBq/μg) ^{177}Lu-DOTATOC (intravenously [i.v.]) at 6 dpi. The effect of virus-mediated SSTR expression on ^{177}Lu-DOTATOC uptake in tumors and normal tissues was evaluated at 6, 24, and 72 h post-RP delivery (Figure 3). Tumor uptake (Figure 3A, left) was increased at all time points in vvDD-SSTR-treated mice compared with control virus or ^{177}Lu-DOTATOC alone and showed statistical significance compared with both control groups at 6 h (1.0% ± 0.13% vs. 0.1% ± 0.05% ID/g, $p < 0.01$, and 0.3% ± 0.1% ID/g, $p < 0.05$, respectively, one-way ANOVA) and ^{177}Lu-DOTATOC at 72 h (0.2% ± 0.04% vs. 0.0% ± 0.0% ID/g, $p < 0.05$, one-way ANOVA). Over the time points evaluated, vvDD-SSTR resulted in an approximately 2.2- to 8.4-fold increase in the mean tumor uptake of radioactivity relative to vvDD-EGFP and a 3.8- to 5.5-fold increase relative to ^{177}Lu-DOTATOC alone. The tumor-to-blood ratio for vvDD-SSTR-treated mice was 37.9 ± 0.6, 143.0 ± 85.4, and 101.6 ± 6.5 at 6, 24, and 72 h, respectively (Figure 3A, right). This was significantly increased relative to vvDD-EFGP and ^{177}Lu-DOTATOC alone-treated mice at 6 h (7.6 ± 4.0 and 5.6 ± 3.6, $p < 0.05$, one-way ANOVA) and 72 h (45.7 ± 11.2 and 22.0 ± 15.5, $p < 0.05$, one-way ANOVA). Normal tissue uptake was generally unaffected by vvDD-directed expression of SSTR (Figures 3B–3D), with a few exceptions. Uptake in the kidneys and ovaries was significantly increased at various time points in mice treated with vvDD-SSTR relative to controls and was likely due to virus infection in these organs. Similarly, other sites where vvDD-SSTR replication was present also displayed transient rises in ^{177}Lu-DOTATOC uptake. However, given the subsequent findings at 24 and 72 h, these are unlikely to be clinically relevant. The ovaries are known to support relatively high levels of vvDD replication in mice.[48] Non-human primate studies have demonstrated no specific ovary tropism with vvDD[49]; therefore, while future studies should closely evaluate for deleterious impacts on ovaries, we believe it is unlikely that further clinical evaluation of vvDD will demonstrate relevant toxicity. While our data showed low levels of virus in the kidneys of vvDD-treated mice (Figures 4B–4D), previous preclinical investigations in immunocompetent murine, rabbit, and non-human primate models have not identified the kidneys as a site of vvDD replication or toxicity.[45,49,50] Therefore, it seems unlikely that the slight increase in kidney radioactivity observed in the vvDD-SSTR + ^{177}Lu-DOTATOC-treated mice would be a toxicity concern in immunocompetent models. That the radioactivity level in kidneys was significantly higher than levels in tumor tissue is certainly a finding to emphasize for further safety evaluations moving forward; however, given the minimal increase in uptake associated with vvDD-SSTR over ^{177}Lu-DOTATOC alone and that renal-protecting agents are standard during the use of PRRT, we believe this should not pose a safety concern. Consistent with vvDD's highly tumor-specific replication (Figure 4), uptake of radioactivity in all other organs was not significantly affected by virus-directed SSTR expression (Figures 3B–3D).

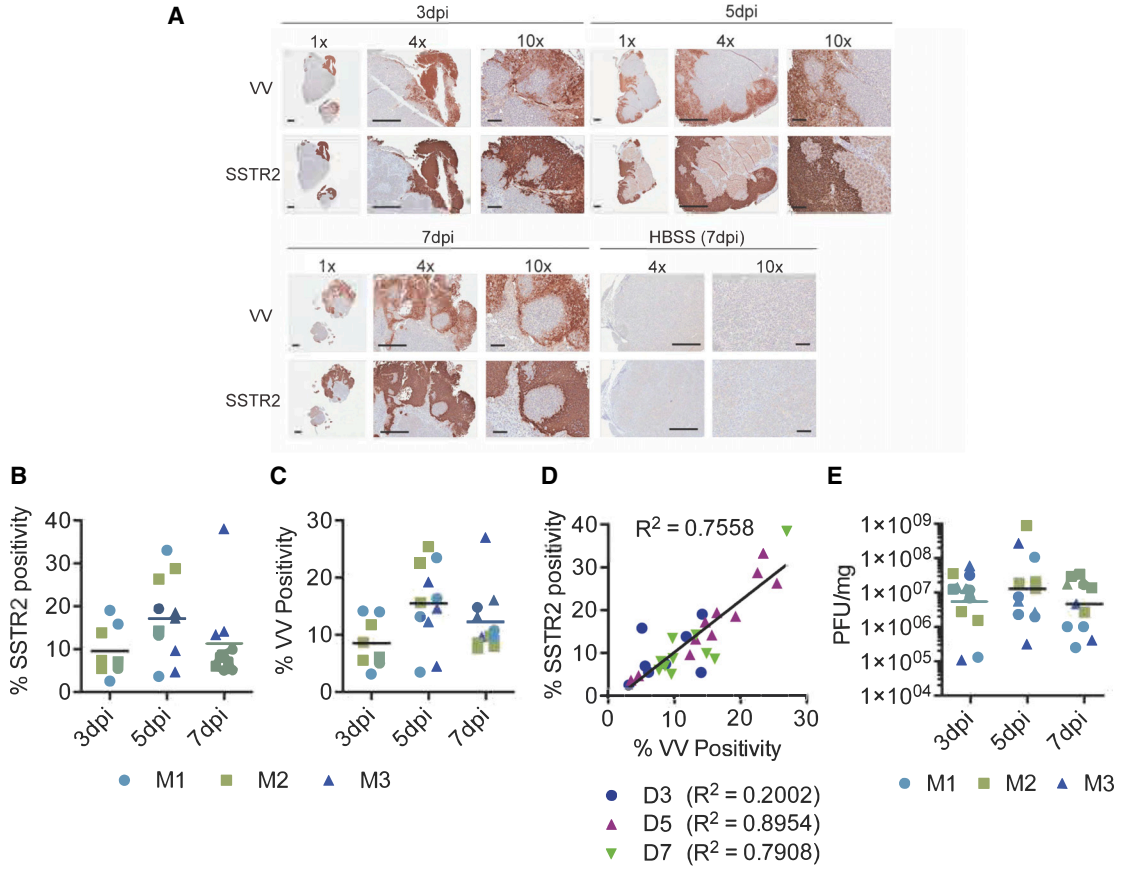

Figure 2. SSTR expression in vvDD-SSTR treated tumor-bearing mice

Tumors (3–4 per mouse) from vvDD-SSTR-treated mice (10^9 PFU; n = 3 per time point) were harvested 3, 5, 7, and 9 dpi and bisected for IHC and virus titering. Formalin-fixed tumor sections were stained with anti-VV and anti-SSTR2 antibodies, while corresponding specimens suspended in HBSS were processed for titering. (A) Representative images of the tumor sections from vvDD-SSTR- and HBSS-treated mice. (B and C) Quantification of IHC staining expressed as the percentage positive pixels relative to total pixels per tumor. (D) Linear correlation between VV and SSTR staining in individual tumors over all time points. (E) Tumor titers as determined by plaque assay. Data points represent the results for individual tumors harvested from each mouse (M1–3) with the overall mean represented by the solid line. Scale bars, 100 μm (10× original magnification) or 500 μm (1–4× original magnification).

Specific uptake of ^{177}Lu-DOTATOC in vvDD-SSTR-infected CRC tumors does not affect virus biodistribution

Tumors and tissues harvested from mice were also used to evaluate virus biodistribution. The effect of ^{177}Lu-DOTATOC on virus in the tumors (Figure 4A) as well as normal tissues (Figures 4B–4D) was evaluated at 24 h (7 dpi), 72 h (9 dpi), and 7 days (13 dpi) post-RP delivery. Consistent with our *in vitro* data, ^{177}Lu-DOTATOC did not decrease virus titers in the tumors or most normal tissues. Interestingly, addition of the RP resulted in a significant increase in tumor titers at 72 h, which was lost by 7 days. Overall, tumor titers were high relative to normal organs (mean titer ±SEM at 24 h, $9.6 \times 10^6 \pm 4.4 \times 10^6$ PFU/mg; 72 h, $2.1 \times 10^7 \pm 6.4 \times 10^6$ PFU/mg; 7 days, $7.8 \times 10^6 \pm 1.6 \times 10^6$ PFU/mg). The ovaries, which are known to support VV replication, showed some of the highest normal tissue titers (mean titer ±SEM at 24 h, $1.4 \times 10^6 \pm 1.1 \times 10^4$ PFU/mg; 72 h, $3.1 \times 10^6 \pm 1.9 \times 10^6$ PFU/mg; 7 days, $4.8 \times 10^5 \pm 4.4$ PFU/mg); however, they were still up to 2 logs lower than tumor titers. Interestingly, a statistically significant decrease in mean virus titer was observed in the ovaries of mice treated with ^{177}Lu-DOTATOC relative to virus alone at 24 h (Figure 4B). This difference was not observed at the later time points and therefore may not reflect a true inhibition of virus replication in ovaries. Alternatively, it may represent a transient decrease in virus replication related to the increased uptake of ^{177}Lu-DOTATOC in the ovaries early after RP injection (Figure 3B). Given the established connection between PRRT and renal toxicity, it is important to evaluate off-target virus replication in the kidneys. Virus was present in the kidneys of all vvDD-SSTR + ^{177}Lu- DOTATOC-treated mice at all time points (mean titer ±SEM at 24 h, $9.1 \times 10^4 \pm 9.1 \times 10^4$ PFU/mg; 72 h, $5.0 \times 10^2 \pm 4.0 \times 10^2$ PFU/mg; 7 days, $6.9 \times 10^3 \pm 6.3 \times 10^3$ PFU/mg). This low level of virus may account for the slightly increased RP uptake observed in the mice treated with vvDD-SSTR + ^{177}Lu-DOTATOC (Figure 3). Finally, non-significant but notable elevations in virus replication were also seen in the spleen, bowel, and pancreas (Figure 4).

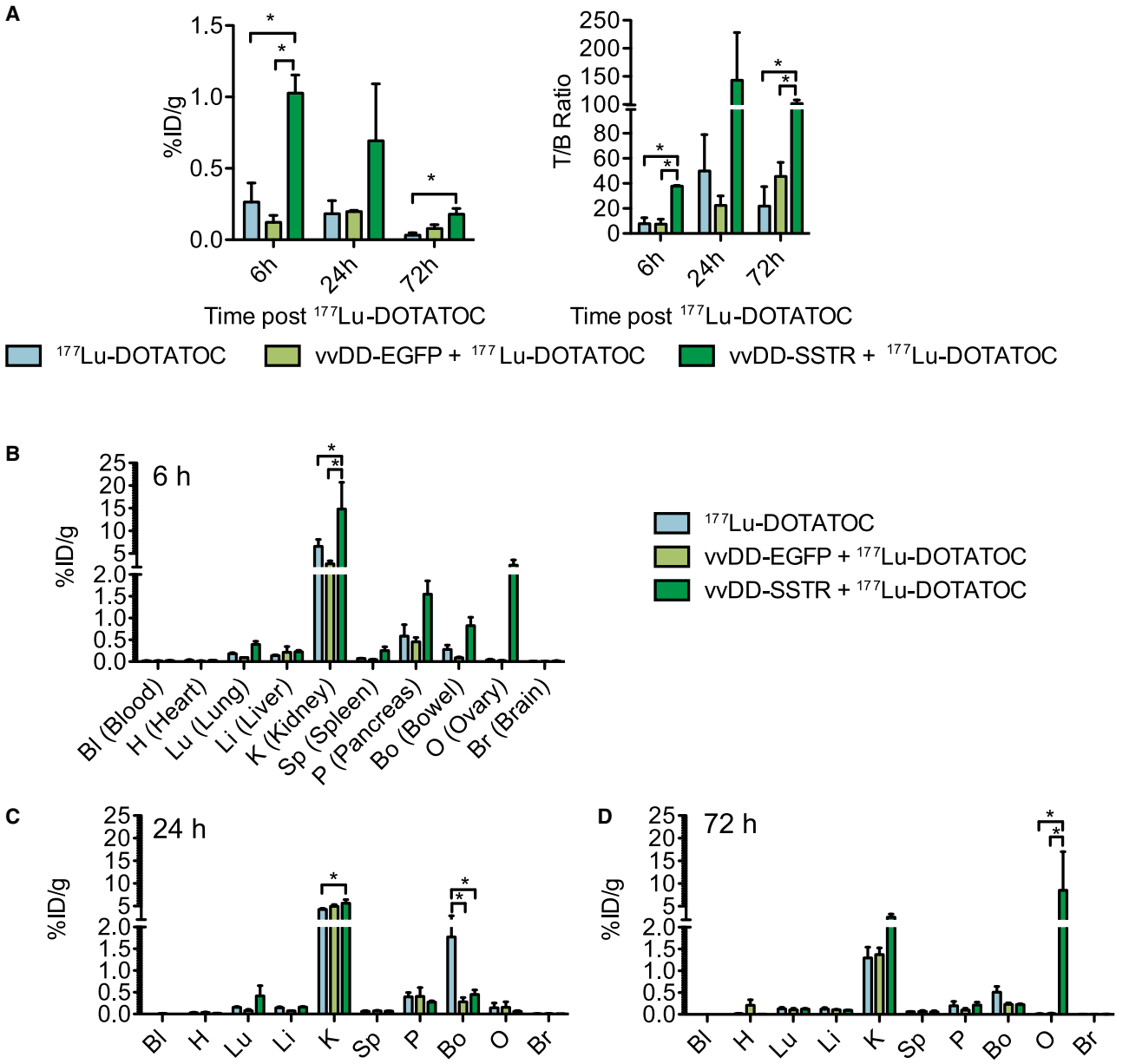

Figure 3. Effect of vvDD-directed SSTR expression on ^{177}Lu-DOTATOC biodistribution

Tumor-bearing mice were treated with vvDD-SSTR or vvDD-EGFP (10^9 PFU) in combination with ^{177}Lu-DOTATOC (3.5 MBq, 29.5–31 MBq/μg) 6 dpi. Tumors (A) and normal tissues (B–D) were harvested at several time points post-RP delivery and analyzed by gamma counting. (A) Tumor uptake and tumor-to-blood ratio. *$p < 0.05$, one-way ANOVA. (B–D) Normal tissue uptake at 6 h (B), 24 h (C), and 72 h (D). *$p < 0.05$, two-way ANOVA. All data are presented as the mean %ID/g ± SEM (n = 3 per time point).

Virus-directed expression of SSTR allows for molecular imaging of intraperitoneal CRC tumors with low endogenous receptor expression

One of the many advantages of using γ-ray-emitting radionuclides is that they can be imaged using standard nuclear imaging modalities such whole-body planar imaging using a gamma-camera or three-dimensional imaging by SPECT/computed tomography (CT). Radionuclides like ^{177}Lu that emit both γ-rays and particulate radiation (β-particles) are therefore valuable for both diagnostic and post-therapy imaging as well as in the actual treatment course. We evaluated the ability of vvDD-directed SSTR expression to lead to sufficient tumor-specific uptake of ^{177}Lu-DOTATOC such that intraperitoneal (i.p.) tumors were imageable by SPECT/CT (Figure 5A). Six hours post-^{177}Lu-DOTATOC administration, tumors from vvDD-SSTR-treated mice were clearly visible by SPECT/CT imaging, whereas no signal was observed in the tumors of vvDD-EGFP-treated mice. Necropsies were performed

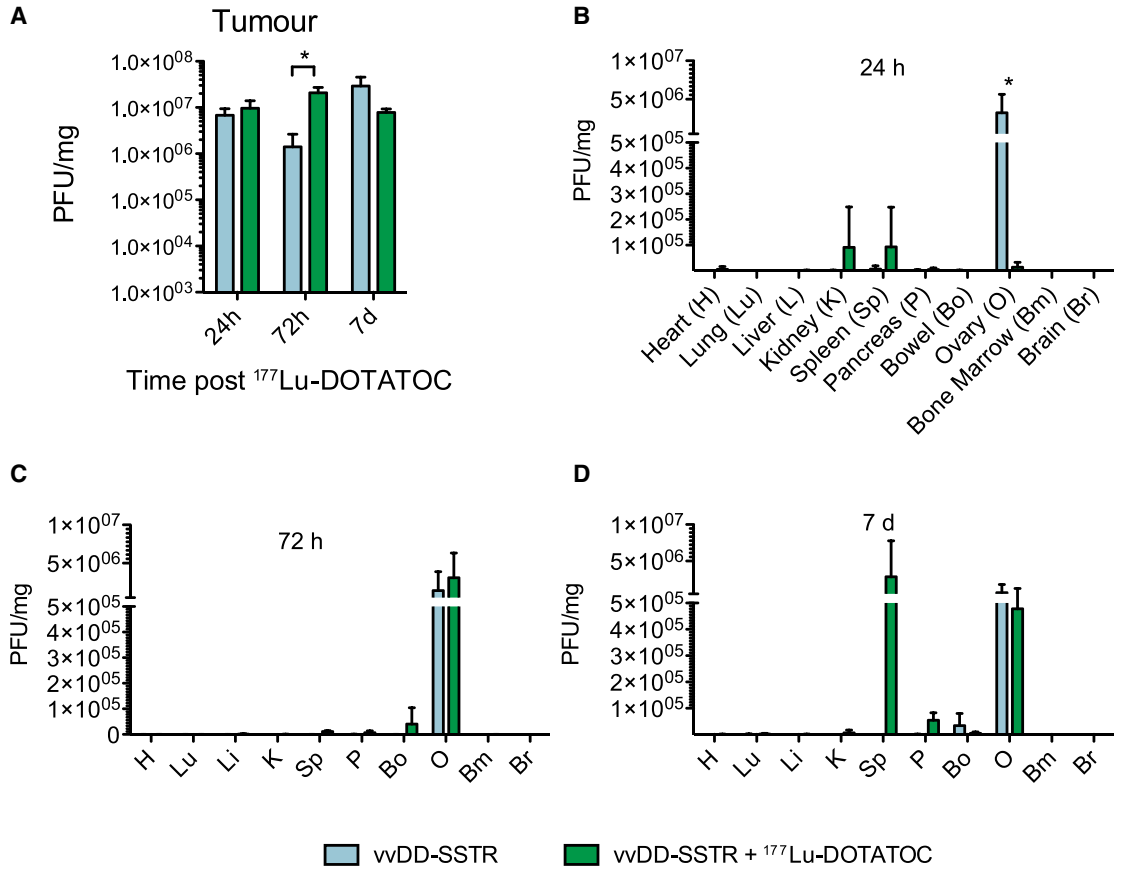

Figure 4. Effect of ^{177}Lu-DOTATOC on vvDD-SSTR2 biodistribution

DLD1 tumor-bearing mice (n = 3 per time point) were treated with vvDD-SSTR (10^9 PFU i.p.) followed by ^{177}Lu-DOTATOC (3.5 MBq i.v.) 6 days later. Tumors (A) and normal tissues (B–D) were harvested and titered by plaque assay. (A) Titers in tumors at 24 h, 72 h, and 7 days post-radiopeptide. *$p < 0.05$, t test (n = 3 per time point). (B–D) Normal tissue titers at 24 h (B), 72 h (C), and 7 days (D) post-radiopeptide administration. *$p < 0.05$, two-way ANOVA with Bonferroni's post-test. All bars represent the mean ± SEM.

immediately following imaging, and white-light images were taken to confirm the location of the tumors. Increased uptake in the tumors of mice treated with vvDD-SSTR was confirmed by gamma-counting (Figure 5B). As expected, kidney uptake was high in both groups, although gamma-counting showed it to be statistically decreased in mice treated with vvDD-SSTR (Figure 5B). This is the opposite effect compared with that observed in the biodistribution studies (Figure 3), where ^{177}Lu-DOTATOC was delivered at approximately 1/10 of the imaging activity but with the same specific activity (29.5–31 MBq/μg). It is possible that kidney uptake was saturated at the higher dose and therefore the small effect attributed to virus-directed SSTR expression observed in the biodistribution studies may be negligible in the context of this high dose. In addition, the tumor-specific expression of SSTR appears to be acting as a tumor sink, leading to decreased kidney uptake in vvDD-SSTR treated mice.

Radiovirotherapy improves survival without toxicity in an orthotopic model of CRC peritoneal carcinomatosis

Tumor-bearing mice were treated with vvDD-SSTR or a receptor-negative control virus (vvDD-EGFP) and/or ^{177}Lu-DOTATOC 6 days later. Radiovirotherapy with vvDD-SSTR was performed at two doses (7.5 and 15 MBq) of ^{177}Lu-DOTATOC, while all control groups received the higher dose (15 MBq). All groups also received the kidney protector D-lysine (2,000 mg/kg). Radiovirotherapy was not associated with any generalized toxicity as determined by total body weight recorded every 1–3 days following ^{177}Lu-DOTATOC up to day 38, at which point all HBSS-treated mice had reached the endpoint (Figure 6A). While the vvDD-SSTR-alone group demonstrated initial substantial weight loss over the first 20 days, given that this temporary finding was not replicated in vvDD-EGFP or either of the combination arms, including vvDD-SSTR, we believe this is not likely to be significant. While it is worth noting, particularly given the known safety profile of vvDD, it is not likely to have meaningful clinical significance. Given that bone marrow toxicity is one of the major concerns associated with cancer therapy, complete blood counts were performed at 8 days post-RP delivery to evaluate the effect of radiovirotherapy on different blood cell compartments (Figure 6B). Radiovirotherapy did not have any myelosuppressive effects at this time point, which corresponds approximately to the maximum drop in white blood cells (WBCs)

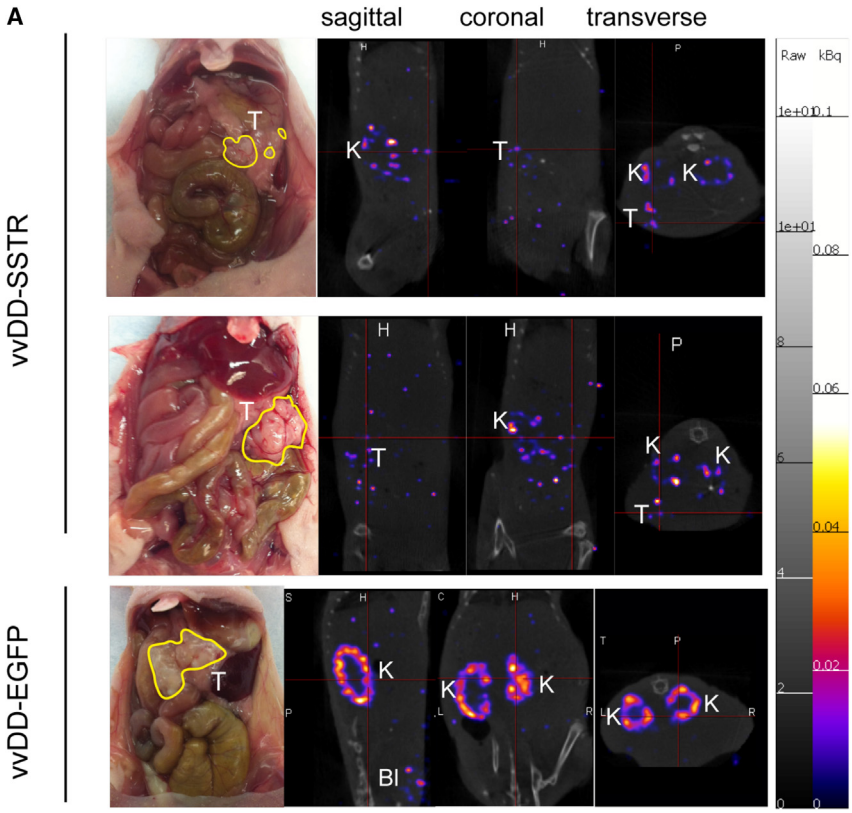

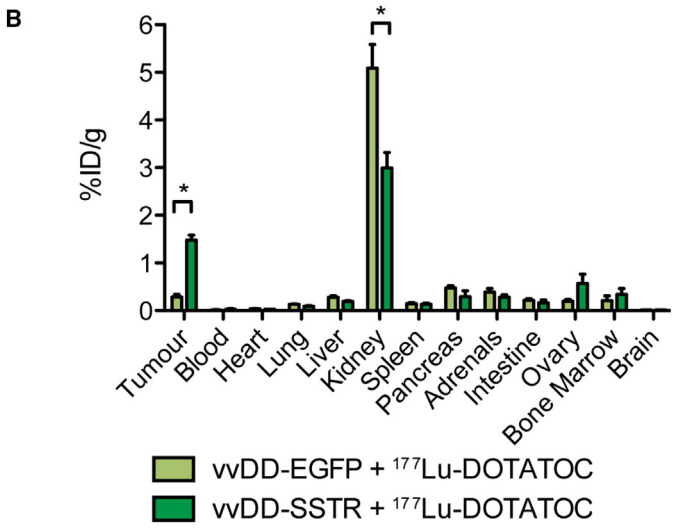

Figure 5. MicroSPECT/CT imaging of intraperitoneal CRC tumors following vvDD-SSTR-directed tumor-specific receptor expression

Tumor-bearing mice were treated with vvDD-SSTR or vvDD-EGFP (10^9 PFU) followed by 37 MBq (29.5–31 MBq/μg) ^{177}Lu-DOTATOC 6 days later. Mice were co-administered D-lysine (2,000 mg/kg) to decrease kidney uptake. (A) Mice were imaged at 6 h post-RP delivery and sacrificed immediately thereafter. White-light images were taken at necropsy to confirm tumor location. The locations of the kidneys (K), tumors (T), and bladder (Bl) are indicated in both the white-light and the SPECT/CT images. (B) Uptake in tumors and normal tissues immediately after imaging was quantified by gamma-counting. Data represent the mean %ID/g ± SEM (n = 3). *p < 0.05 two-way ANOVA with Bonferroni's post-test.

reported in rats treated with ^{177}Lu-DOTATATE.[51] Given that radiovirotherapy was well tolerated in this model, we then evaluated the effect of treatment on overall survival (Figure 6). The median survival in all treatment groups was increased relative to the HBSS-treated controls (38 days median survival) and was statistically significant in all cases, with the exception of vvDD-EGFP + ^{177}Lu- DOTATOC (15 MBq) (55 days median survival), which showed a trend toward improvement.

The addition of ^{177}Lu-DOTATOC to vvDD-SSTR significantly improved the median survival relative to virus alone when administered at 15 MBq (median survival 70 vs. 40 days, p = 0.0498), but not at 7.5 MBq (median survival 51 vs. 40 days, p = 0.365). This shows that there is a dose effect wherein the high-dose (15 MBq) ^{177}Lu-DOTATOC treatment was significantly more effective than the low dose (7.5 MBq) when given in combination with the SSTR-expressing virus (median survival 70 vs. 51 days, p = 0.0467). There was no significant improvement in survival between mice treated with vvDD-EGFP alone or in combination with 15 MBq ^{177}Lu-DOTATOC (median survival 47.5 vs. 55 days, p = 0.256), demonstrating that radiovirotherapy was receptor expression specific (Figure 6).

DISCUSSION

PRRT using ^{177}Lu-labeled SS analogs is an effective treatment option for patients with SSTR-positive NETs. In patients with inoperable disease, PRRT has resulted in a 3–6 year increased survival benefit from the time of diagnosis compared with historically reported data.[5] Currently, radiolabeled SS analogs represent the only class of RPs approved for use in North America.[52] Metastatic NETs, particularly carcinoid malignancies, often occur in some of the same anatomical locations common to metastasized CRC, including the peritoneum, liver, and lungs.[53] In both patient populations, complete surgical resection is one of the best prognostic indicators,[54,55] but,

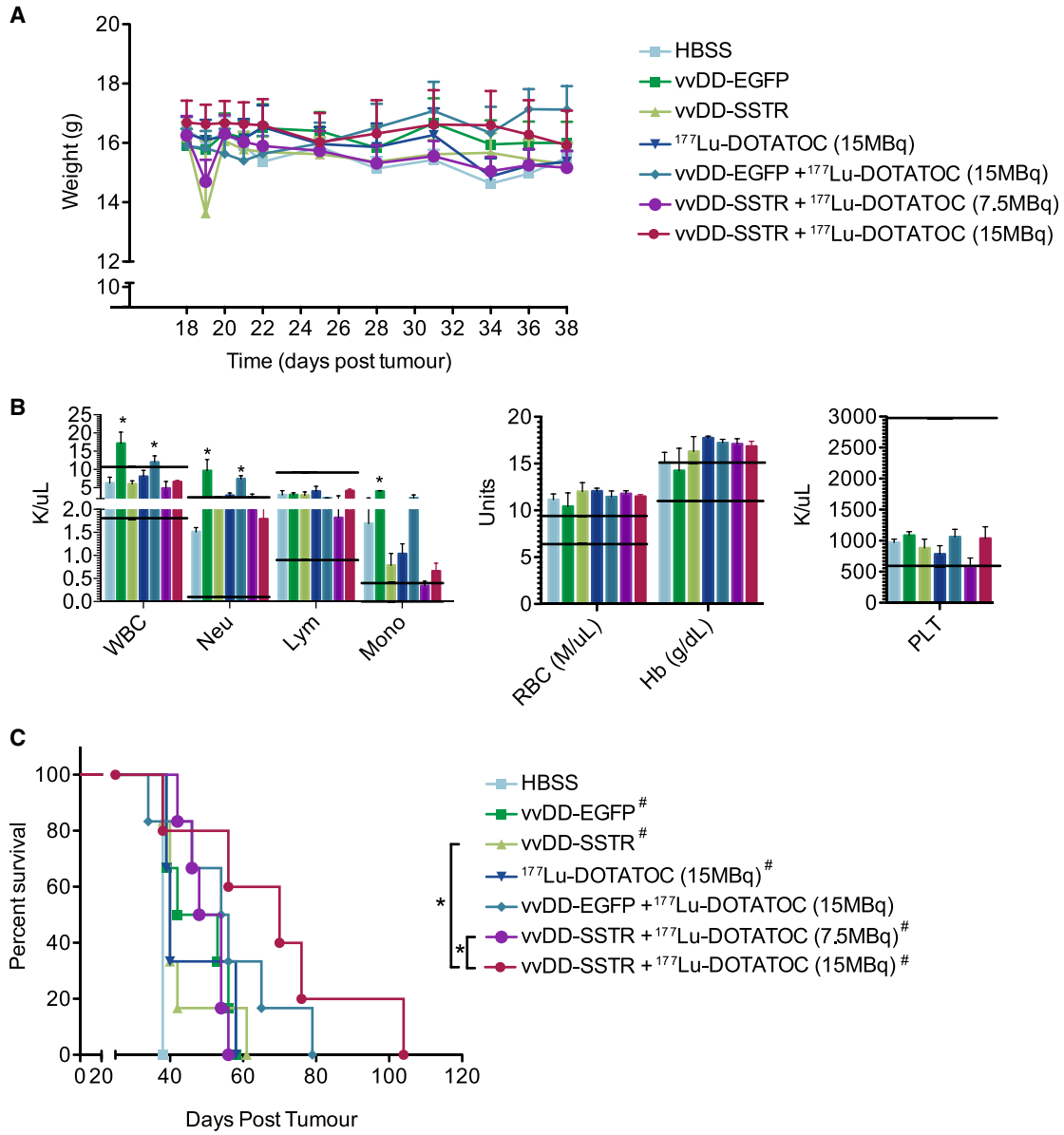

Figure 6. Radiovirotherapy toxicity and efficacy in an orthotopic model of metastatic colorectal cancer

Tumor-bearing mice were treated with virus (10^9 PFU i.p.) on day 12 followed by ^{177}Lu-DOTATOC (7.5 or 15 MBq i.v.) 6 days later. (A) Total body weight over time was monitored for signs of toxicity. (B) Complete blood counts were performed 8 days post-RP. *$p < 0.05$ relative to HBSS, one-way ANOVA (n = 3). Horizontal lines represent the lower and upper threshold of the normal range for each measurement. (C) Kaplan-Meier survival curves were compared to evaluate the efficacy of treatment. Median survivals were 38 days (HBSS, n = 3), 47 days (vvDD-EGFP, n = 6), 40 days (vvDD-SSTR, n = 6), 40 days (^{177}Lu-DOTATOC, 15 MBq, n = 3), 55 days (vvDD-EGFP + ^{177}Lu-DOTATOC, 15 MBq, n = 6), 51 days (vvDD-SSTR + ^{177}Lu-DOTATOC, 7.5 MBq), and 70 days (vvDD-SSTR + ^{177}Lu-DOTATOC, 15 MBq). #$p < 0.05$ compared with HBSS group, *$p < 0.05$ compared with vvDD-SSTR + ^{177}LuDOTATOC (15 MBq), log-rank test.

unfortunately, for a large population of patients with metastatic disease, complete resection is not an option. One of the major factors precluding patients from surgery is the proximity of a tumor to critical organs and structures; similarly, this makes external beam radiation therapy and brachytherapy mostly untenable in these patients, due to significant toxicity concerns. In the case of SSTR-expressing NETs, inoperable tumors can be effectively controlled by targeted radiotherapy using systemically administered radiolabeled SS analogs. Given the success of PRRT in controlling advanced and metastatic disease, we and others have proposed the use of receptor-encoding OVs to direct tumor-specific receptor expression, thereby making cancers with low endogenous receptor expression amenable to PRRT.[8,10,13–17,34,36,37,41,56–63]

In this study we hypothesized that vvDD expressing the human SSTR (subtype 2A) would lead to specific accumulation of the radiolabeled SS-analog ^{177}Lu-DOTATOC in receptor-negative CRC tumors, leading to improved survival in an orthotopic xenograft model. Our results confirmed that virus-directed receptor expression led to specific uptake of the RP in tumors, with minimal effect on the normal tissue biodistribution, as determined by both *ex vivo* quantification of tissue radioactivity and non-invasive SPECT/CT imaging. Furthermore, we report a $\geq$20 day improvement in the median survival of mice treated with vvDD-SSTR and ^{177}Lu-DOTATOC (15 MBq) compared with all other groups. The only other study investigating OV delivery of SSTR combined with a radiolabeled SS analog (^{90}Y-DOTATOC) with the intent to treat was performed in nude mice bearing subcutaneous non-small cell lung tumors.[11] In that study, mice were treated intratumorally with an SSTR2-expressing adenovirus followed by RP 2 dpi at radioactivities (400–500 μCi; 14.8–18.5 MBq) comparable to that used in our treatment studies. The treatment course differed in that their mice received two injections of the RP 2 days apart, followed by a second treatment cycle repeated 7 days later. The tumor uptake observed in our biodistribution study following vvDD-SSTR treatment (1.03% ± 0.12% ID/g 24 h post-RP) was similar to that reported by Rogers et al. following ^{111}In-DTPA-D- Phe1-octreotide administration in AdSSTR2-treated mice (1.3% ± 0.7% ID/g 48 h post-RP).[11] They also reported a significant delay in the time to tumor quadrupling in mice treated with radiovirotherapy compared with ^{90}Y-DOTATOC alone and untreated controls; however, the effect of virus alone was not evaluated. Studies that look at ^{177}Lu-DOTATATE uptake in mouse models of subcutaneous SSTR-positive small cell lung or carcinoid tumors have reported moderately (3.7% ± 0.99% ID/g)[64] or substantially (17% ± 3% ID/g)[65] increased uptake, respectively, compared with that reported here. This likely has to do with differences in the density of receptor expression on the surface of the various cell lines relative to that achieved by virus infection.

Despite the clear benefit of combination vvDD-SSTR and ^{177}Lu-DOTATOC radiovirotherapy, all mice were eventually sacrificed as a result of tumor growth. This indicates that there is still room for improvement in the design and implementation of this radiovirotherapy strategy. There are several modifications to the treatment regimen that warrant further investigation, the first being to increase the activity of the ^{177}Lu-DOTATOC administered. Previous studies in xenograft models of SSTR-positive NETs have demonstrated efficacy and safety with doses up to 30 MBq.[65] Furthermore, nephrotoxicity profiling in nude mice receiving ^{177}Lu-DOTATATE suggests that we may be able to administer doses much higher than 30 MBq,[66] particularly considering that ^{177}Lu-DOTATOC appears to have slightly lower renal uptake relative to ^{177}Lu-DOTATATE.[67]

While it is the case that replicating OVs are capable of much greater spread than their non-replicating counterparts and therefore result in significantly increased tumor uptake of radioligands,[22] incomplete tumor infection remains a challenge to effective OV monotherapy. Low density and heterogeneity of receptor expression have been identified as a critical limitation to effective PRRT of SSTR-positive NETs, due to non-homogeneous delivery and insufficient uptake of the RP throughout the tumor volume.[68] The IHC analysis presented here revealed heterogeneous SSTR expression corresponding to areas of VV staining throughout the tumors of vvDD-SSTR-treated mice (Figure 2). Furthermore, there was substantial variation in the extent of infection and therefore receptor expression between individual tumors harvested from the same mouse, as has previously been reported with vvDD in similar mouse models.[45] The heterogeneous distribution of virus-mediated receptor expression in these studies may have limited the maximum effect achievable with 15 MBq of ^{177}Lu-DOTATOC had receptor expression been more homogeneous. Accordingly, strategies to specifically increase the uniformity of receptor expression and overall uptake in the tumors (but not normal tissues) would likely improve the therapeutic efficacy of radiovirotherapy. A previous study using an NIS-expressing adenovirus combined with radioiodide demonstrated that this could be achieved by increasing the virus dose administered,[59] which presumably increased the level of receptor expression in the tumor. However, in the context of VV OV therapy, doses above 10^9 PFU (the dose used in our studies) may not be tolerable in immunosuppressed mice and are near the top threshold of achievable titers under clinical manufacturing conditions. Therefore, increasing virus-mediated receptor expression through other means, such as improving virus delivery and/or spread in tumors, could have a meaningful impact on the density and distribution of receptor expression within the tumor. For example, cell carriers have been used to mask systemically delivered (i.p. or i.v.) virus from immune neutralization and thereby improve virus delivery,[69] while modified OVs encoding proteins involved in extracellular matrix (ECM) degradation or enhancing cell-cell fusion demonstrate more efficient spread through tumors.[70] It is likely that a cell carrier would improve delivery of vvDD-SSTR in our model, as they have been shown to significantly increase vvDD delivery to i.p. CRC tumors, an effect that was further enhanced by the addition of immunosuppressive drugs.[71] Strategies to improve spread have also proved effective with VV, wherein a recombinant Lister strain virus encoding the ECM degrading enzyme metalloproteinase (MMP)-9, resulted in increased virus spread and improved tumor growth inhibition in a subcutaneous tumor model.[72]

Translation of preclinical radiovirotherapy studies to the clinic demands careful consideration of issues related to potential toxicity. The primary organs of concern in radiotherapy in general, and PRRT specifically, are the kidneys, bone marrow,[73,74] and ovaries.[75] Liver toxicity has been observed in some PRRT clinical trials, although this is generally attributed to the presence of liver lesions.[5] In addition to the expected off-target sites of radiation toxicity, it is important to also consider the off-target sites of virus replication, as virus-directed receptor expression may lead to RP uptake in these tissues. The biodistribution studies presented here demonstrate receptor-dependent increases in ^{177}Lu-DOTATOC uptake in the kidneys (at 6 and 24 h) and ovaries (at 72 h) of vvDD-SSTR-treated mice (Figure 3). Of note, receptor-independent uptake also appears to be present. Our virus biodistribution data, which are consistent with previously published results in similar models,[45,76] showed low levels of

virus in the kidneys at all time points and ovary titers approximately 10-fold lower than tumor titers. Occasionally we have seen virus persistence in the spleen, and we attribute it to the fact that there are replicating cells in the spleen following virus infection, and VV infection of cells is not cell specific. When the kidney protectant D-lysine was co-administered with ^{177}Lu-DOTATOC (37 MBq) for the imaging studies, we observed a decrease in the mean kidney percentage of injected dose per gram of tissue (%ID/g) uptake from mice treated with vvDD-SSTR relative to the receptor-negative control virus (Figure 5B). It is widely recommended that patients undergoing SSTR-directed PRRT also receive some sort of kidney-protecting agent (e.g., lysine, arginine, or an amino acid mixture); therefore, based on our data it seems unlikely that virus-directed receptor expression would lead to any increased risk of renal toxicity. Mouse ovaries are consistently shown to be an off-target site of VV replication by mechanisms that are not entirely understood.[48] Nevertheless, it is important to be aware that this organ tropism has not been observed in non-human primate studies,[49] nor has ovarian toxicity been reported in any clinical trials (although to date it has not been looked at specifically). Therefore, while the murine data may be an impetus to directly evaluate this in future clinical studies, it likely represents a murine-specific phenomenon and consequently any virus receptor-driven ovarian toxicity is unlikely to extend beyond preclinical mouse models. That being said, the ovaries are a common site of implantation in patients with colorectal PC,[77] and virus-directed uptake in this organ could be beneficial to therapy.

SS analogs have the advantage of being amenable to labeling with a variety of radionuclides with different physical and biological properties. In the context of radiovirotherapy, which relies primarily on the cross-fire effect, the radionuclide must have sufficient tissue-penetrating capacity to deposit its energy multiple cell diameters from its source, as is the case of β emitters such as ^{177}Lu, ^{90}Y, or ^{188}Re, which have a maximum range of 2, 3, and 12 mm in tissue, respectively. Weighing the benefits of the desired cross-fire effect within the tumor against the risks associated with the undesired cross-fire effect in normal tissues has led to more frequent use of ^{177}Lu- and ^{90}Y-labeled SS analogs (although others have also been investigated). Previous work performed in tumor-bearing rats suggests that using a ^{90}Y/^{177}Lu-DOTATATE cocktail may have better tumor control activity in disease models with multiple tumors of varying sizes.[1] Recent clinical studies provide further evidence that a ^{90}Y/^{177}Lu-DOTATATE cocktail may be more efficacious[78] and less toxic[79] than a single RP. Radionuclide cocktails may be similarly beneficial to radiovirotherapy of peritoneally disseminated CRC, which is characterized by many tumors over a range of sizes (microscopic to >5 cm in diameter) in a single patient.

In this study, SPECT imaging was feasible due to the γ-photons emitted during ^{177}Lu decay. That said, relative to other γ-emitting radionuclides, ^{177}Lu is not the best suited to SPECT imaging due to the low abundance of imageable γ-photons. ^{111}In-DOTATOC represents an ideal agent for SPECT imaging as a result of the two high-abundance γ-photons emitted during ^{111}In decay. Alternatively, imaging of vvDD-SSTR-directed DOTATOC uptake could also be achieved using a ^{68}Ga-labeled peptide in conjunction with positron emission tomography (PET) imaging. This has the advantage of allowing for much higher imaging sensitivity and therefore a more accurate representation of the tissue uptake biodistribution.

In addition to the cross-fire effect, both targeted radiotherapy and VV therapy have been shown to induce biological bystander effects,[80–82] which are thought to be influential in mediating their respective antitumor activities. There is a growing body of evidence indicating that immunological mechanisms underlie the abscopal effects observed in radiation therapy of metastatic disease and that this effect can be bolstered by pretreatment with immunologic preparations (e.g., activated dendritic cells [DCs], IL-2, active macrophage inflammatory protein 1α [MIP-1α], Toll-like receptor [TLR]).[83] For example, studies have shown that type I interferons (IFNs) can have a radiosensitizing effect in various cancer cell lines, including human CRC cells.[84] As well, cytokines produced by activated CD4$^+$ T cells were also found to sensitize tumor cells to γ-irradiation.[85] OVs are in part a type of immunotherapy, and the biological bystander effect induced by OVs, which consists primarily of intracellular and secreted "danger signals," antiviral cytokines, chemokines, and activated immune cells,[86] closely resembles the tumor microenvironment that has been shown to improve the anti-tumor effects of radiation therapy. Therefore, it is perhaps not surprising that therapeutic efficacy has been improved by the combination of many OVs,[20] including VV,[87–89] with radiation therapy. This bystander effect could be further exploited in the radiovirotherapy approach by using a virus expressing an immunomodulatory protein that has been shown to sensitize cells to radiation.

To date, the vast majority of radiovirotherapy studies have looked at virus delivery of human NIS with subsequent ^{131}I treatment.[63] Currently, there are several early phase (I/II) clinical trials designed to evaluate the safety of an NIS-encoding measles virus as well as our ability to non-invasively track virus gene expression by SPECT/CT imaging. The results of these studies, most of which are still in the recruiting stage, will determine whether future trials will include a radiovirotherapy study arm.

Oncolytic VV shows specific and robust replication in a broad range of tumor cell types;[25] therefore, oncolytic VV-directed SSTR expression combined with PRRT could have widespread applicability beyond CRC. The results presented here support the investigation of this treatment approach in other models with the objective of clinical translation. Specifically, a more detailed examination of the long-term effects of vvDD-SSTR and targeted radiotherapy on the kidneys is necessary to confirm there is no reasonable expectation of increased renal toxicity risk in patients. Two recently published phase I clinical trials have demonstrated the safety and tumor specificity of western reserve vvDD, including in patients with CRC,[30,32] representing a promising step forward toward the future clinical translation of its SSTR-expressing counterpart. Zeh et al.[30] demonstrated safe intratumoral administration of vvDD at doses up to 3×10^9 PFU and further

reported clinical benefit in one melanoma patient leading to subsequent complete surgical resection of their tumor with negative margins. Downs-Canner and colleagues demonstrated safe i.v. vvDD administration at doses up to 3×10^9 PFU, with no dose-limiting toxicities or severe adverse events, tumor-specific viral replication, and clinical response in a subset of patients.[32] In future trials, the use of vvDD-SSTR would have the advantage of allowing for non-invasive monitoring of virus biodistribution through molecular imaging and would pave the way for later investigation of radiovirotherapy with radiolabeled SS peptides.

MATERIALS AND METHODS

Cell lines, virus, and reagents

Human colorectal adenocarcinoma (DLD1) and monkey kidney fibroblast (CV-1) cell lines were obtained from the American Type Culture Collection (ATCC; Manassas, VA, USA). The 24-JK murine sarcoma cell line was obtained from the National Institutes of Health (Bethesda, MD, USA). Cells were cultured in Dulbecco's modified Eagle medium (DMEM; Sigma Aldrich, St. Louis, MO, USA) supplemented with 10% (v/v) fetal bovine serum (FBS; PAA Laboratories, Etobicoke, ON, Canada) and 1% antibiotic-antimycotic (Invitrogen, GIBCO, Grand Island, NY, USA) at 37°C with 5% CO_2. The previously described thymidine kinase (*tk*) and vaccinia growth factor (*vgf*)-deleted VV (vvDD) expressing the human SSTR subtype 2A[10] and control vvDD expressing EGFP or RFP[48] were propagated in 24-JK cells and purified by ultracentrifugation over a sucrose cushion. Virus stocks were stored at −80°C and titered on CV-1 cells.[90] D-lysine (Sigma Aldrich) was dissolved in PBS to a concentration of 200 mg/mL and filter sterilized using a 0.22 μm pore syringe filter immediately prior to administration.

Peptide labeling

All chemicals were obtained from commercial sources and used without further purification. DOTA-conjugated D-Phe1-[Tyr3]-octreotide (DOTATOC; American Peptide, Sunnyvale, CA, USA) was radiolabeled with $^{177}LuCl_3$ (PerkinElmer, Waltham, MA, USA) as previously reported.[91] The radioconjugate was obtained in >99% radiochemical purity at a specific activity of 42–44 MBq/nmol DOTA-peptide (29.5–31.0 MBq/μg).

In vitro virus infections and plaque assays

Cells were infected at a low volume (400 μL) in 2.5% DMEM for 2 h with shaking every 10 min, after which DMEM with 10% FBS was added to the wells. Plaque assays were performed on harvested cells and tissues to quantify live virus. Tissue samples were frozen in HBSS and stored at −80°C until use and then were homogenized using a TissueLyzer II (Qiagen, Hilden, Germany) and exposed to three freeze-thaw cycles and sonication prior to titering on CV-1 cells. For titering, infected CV-1 cells were incubated for 48 h prior to staining with crystal violet[92] and quantitation of the PFU per milliliter. For quantification of virus in tissues as mentioned above, titers were normalized to the total protein per sample as determined by a Pierce bicinchoninic acid (BCA) protein assay kit (Thermo Fisher Scientific, Waltham, MA, USA).

In vitro cell viability

Cells were seeded at 1×10^4 per well in a 96-well plate and incubated overnight. Cells were infected with vvDD-SSTR or vvDD-RFP as above and incubated for 24 h. Supernatant was removed and cells were incubated with ^{177}Lu-DOTATOC (37–740 kBq; 1.2–25 ng) diluted in 10% DMEM for 4 h. Unbound ^{177}Lu-DOTATOC was removed, wells were washed twice with PBS, and medium was added. Seventy-two hours later, cell viability was assessed by 3-(4,5-dimethyl-2-yl)-5-(3-carboxymethoxyphenyl)-2-(4-sulfophenyl)-2H-tetrazolium (MTS) assay (CellTiter96 Aqueous One Solution, Promega, Madison, WI, USA) according to the manufacturer's protocol.

Virus replication in the presence of ^{177}Lu-DOTATOC

Cells were seeded at 5×10^5 per well (six well plate) and incubated overnight. Cells were infected at an MOI of 0.1 for 24 h prior to a 4 h incubation with increasing activities of ^{177}Lu-DOTATOC (1–20 μCi; 1.2–25 ng) diluted in 10% DMEM. Wells were washed twice with PBS to remove any unbound ^{177}Lu-DOTATOC, supplemented with 10% DMEM, and incubated for the indicated times. The entire contents of the wells (cells and supernatant) were collected by cell scraping every 24 h beginning at baseline (after RP incubation). Samples were titered on CV-1 cells immediately following their harvest.

Combination index

Dose-response curves generated from the cell viability data were analyzed using the Chou and Talalay method for quantifying drug-drug interactions.[47] Experiments were performed using non-fixed dose ratios. Data are presented in a normalized isobologram where (D)1,2 is the dose required to achieve a given fraction when drug 1 or 2 is administered separately, and (Dx)1,2 is the dose required to achieve the same fraction affected when drugs 1 and 2 are administered in combination. On the (D)1/(Dx)1 vs. (D)2/(Dx)2 plot (normalized isobologram), synergy is defined as data points falling below the line connecting the points (0, 1) and (1, 0). Data points falling on this line represent additive interactions, while those above the line indicate antagonism.

Mice

Six- to eight-week old female BALB/c nude mice (C.Cg/AnNTac-*Foxn1nu* NE9; Taconic Farms, NY, USA) were housed under standard conditions and given food and water *ad libitum*. Experiment protocols were approved by the Animal Care Committee (UHN, Toronto, ON, Canada). Survival endpoint criteria as defined by the Animal Care Committee included severe abdominal distension resulting in decreased mobility and/or cachexia. Mice were injected i.p. with 5×10^6 DLD1 on day 0 followed by virus (10^9 PFU i.p.) suspended in HBSS + 0.1% bovine serum albumin (BSA) or vehicle alone on day 12. To evaluate the expression SSTR in i.p. tumors, groups of vvDD-SSTR-treated mice (n = 3) were sacrificed at 3, 5, 7, and 9 dpi, and tumors (up to five per mouse) were harvested, bisected, and processed as described for IHC and titering. For the biodistribution study, tumor-bearing mice (n = 3 per time point) were treated with vvDD-SSTR, vvDD-EGFP, or vehicle alone (day 12) followed by 3.5 MBq ^{177}Lu-DOTATOC i.v. on day 18. Imaging was performed on

mice (n = 3) treated with vvDD-SSTR or vvDD-EGFP in combination with 37 MBq ^{177}Lu-DOTATOC. For the treatment study, mice were divided into six groups: vehicle alone, ^{177}Lu-DOTATOC, vvDD-EGFP, vvDD-EGFP + ^{177}Lu-DOTATOC, vvDD-SSTR + ^{177}Lu-DOTATOC (low dose), and vvDD-SSTR + ^{177}Lu-DOTATOC (high dose). Radiovirotherapy was evaluated at two ^{177}Lu-DOTATOC doses (7.5 and 15 MBq) in the vvDD-SSTR-treated mice and at the higher dose (15 MBq) in all control groups. For both the imaging and the treatment studies, D-lysine was used to minimize kidney uptake. Mice received four i.p. injections of D-lysine (2,000 mg/kg per injection) once every hour, beginning 30 min prior to RP injection.

Immunohistochemistry and histopathology

Staining was performed on tissues fixed in 10% buffered formalin for 72 h followed by 70% ethanol. Samples were paraffin embedded, sectioned, and stained using rabbit monoclonal anti-SSTR subtype 2 [UMB1] (ab134152, 1/800; Abcam, Cambridge, MA, USA) or polyclonal rabbit anti-VV (ab35219, dilution 1/1000; Abcam, Cambridge, MA, USA) primary antibodies and horseradish peroxidase (HRP)-labeled secondary antibodies. Stained slides were scanned using ScanScope XT (Aperio Technologies, Vista, CA, USA), and staining was quantified using ImageScope's Positive Pixel algorithm (Aperio Technologies), where % positivity represents the percentage of positively staining pixels relative to the total number of pixels in a defined area. Defined areas were manually drawn around each tumor. Kidneys from the treatment study were stained using a standard H&E protocol and evaluated for toxicity by a blinded veterinary pathologist.

Biodistribution studies

Mice were sacrificed at selected time points post-RP injection, and blood (collected via cardiac puncture) and tissues (tumor, heart, lung, liver, kidney, spleen, pancreas, adrenal gland, bowel, ovary, bone marrow, and brain) were harvested. Up to five tumors per mouse were removed (depending on the number of tumors present). Individual tumors and normal tissues were bisected, with one-half stored in HBSS at −80°C for virus quantification by plaque assay (all tissues except blood) and the other half placed in preweighed scintillation vials for quantification of ^{177}Lu activity.

Gamma counting

Tissues were weighed, and activity was measured in a gamma-counter (PerkinElmer Wizard 1480 Wizard 3″, Waltham, MA, USA) along with a standard of the injected dose, such that decay-corrected uptakes were calculated as the percentage of the injected dose per gram of tissue (%ID/g). The total injected dose per mouse was equal to the difference between the pre- and the post-injection syringe radioactivity determined by a CRC-15R dose calibrator (Caointec, Ramsay, NJ, USA).

MicroSPECT/CT imaging

Mice were imaged 3–6 h post-^{177}Lu-DOTATOC injection. Mice were anesthetized by inhalation of 2% isoflurane in O_2. Imaging was performed on a NanoSPECT/CT tomograph (BioScan, Washington, DC) equipped with 4NaI(Tl) detectors and fitted with 1.4 mm multi-pinhole collimators (resolution <1.2 mm at full width at half-maximum). Photons were accepted from the 10% windows centered on lutetium's three photopeaks at 208, 113, and 245 keV. Projections were acquired in a 256 × 256 acquisition matrix for a total of 60 min. Images were reconstructed using an ordered-subset expectation maximization (OSEM) algorithm (nine iterations). Cone beam CT images were acquired (180 projections, 1 s/projection, 45 kVp) before microSPECT images. MicroSPECT and CT images were co-registered using InVivoScope software (Bioscan/inviCRO, Boston, MA, USA). Mice were sacrificed immediately following imaging, and necropsies were performed to confirm the location of i.p. tumors. Normal and tumor tissues were then harvested for gamma-counting as in the biodistribution studies.

Treatment and toxicity studies

Tumor-bearing mice were treated with virus (10^9 PFU) and/or ^{177}Lu-DOTATOC (7.5 or 15 MBq). Cages were changed 24 h after RP administration. Mice were weighed every 2–3 days and followed for signs of toxicity or disease progression. Saphenous vein blood was collected from three mice per group at 8 days post-RP for analysis. Complete blood counts were performed using a HEMAVET multispecies hematology analyzer (Drew Scientific, Dallas, TX, USA). When mice reached the defined endpoint they were sacrificed, and kidneys were collected and fixed in formalin for histopathology.

Data availability

All raw data pertaining to this study are stored ether digitally on an external hard drive or in hard copy in the McCart lab. These are available upon request.

ACKNOWLEDGMENTS

This work was supported by a Canadian Institutes of Health Research (CIHR) operating grant (MOP-84208) and a Terry Fox New Frontiers Program project grant (TFF-122868). K.O.-P. was supported by a CIHR Banting and Best Doctoral Award. The authors would also like to acknowledge the contributions of Dr. Nan Tang to this work.

AUTHOR CONTRIBUTIONS

K.O.-P. conducted the bulk of the experiments described herein, as well as manuscript writing, with assistance from D.M., C.S., S.A.A., and F.A.A. J.A.M. was the primary investigator for the work, designing the research with K.O.-P. and directing its execution. L.O. acted as laboratory technician, assisting with experimental and laboratory logistics. D.S. and M.G. provided assistance and expertise with those portions of the work involving radiation therapy and imaging. R.R. provided assistance and expertise specifically regarding radiotherapy pharmacology.

DECLARATION OF INTERESTS

The authors declare they have no competing interests.

REFERENCES

1. de Jong, M., Breeman, W.A.P., Kwekkeboom, D.J., Valkema, R., and Krenning, E.P. (2009). Tumor imaging and therapy using radiolabeled somatostatin analogues. Acc. Chem. Res. *42*, 873–880.
2. Kong, G., and Hicks, R.J. (2019). Peptide receptor radiotherapy: current approaches and future directions. Curr. Treat. Options Oncol. *20* (10), 77.
3. Hamiditabar, M., Ali, M., Roys, J., Wolin, E.M., O'Dorisio, T.M., Ranganathan, D., Tworowska, I., Strosberg, J.R., and Delpassand, E.S. (2017). Peptide receptor radionuclide therapy with 177Lu-octreotate in patients with somatostatin receptor expressing neuroendocrine tumors: six years' assessment. Clin. Nucl. Med. *42*, 436–443.
4. Mirvis, E., Toumpanakis, C., Mandair, D., Gnanasegaran, G., Caplin, M., and Navalkissoor, S. (2020). Efficacy and tolerability of peptide receptor radionuclide therapy (PRRT) in advanced metastatic bronchial neuroendocrine tumours (NETs). Lung Cancer *150*, 70–75.
5. Kwekkeboom, D.J., de Herder, W.W., Kam, B.L., van Eijck, C.H., van Essen, M., Kooij, P.P., Feelders, R.A., van Aken, M.O., and Krenning, E.P. (2008). Treatment with the radiolabeled somatostatin analog [177 Lu-DOTA 0,Tyr3]octreotate: toxicity, efficacy, and survival. J. Clin. Oncol. *26*, 2124–2130.
6. van Essen, M., Krenning, E.P., Kooij, P.P., Bakker, W.H., Feelders, R.A., de Herder, W.W., Wolbers, J.G., and Kwekkeboom, D.J. (2006). Effects of therapy with [177Lu-DOTA0, Tyr3]octreotate in patients with paraganglioma, meningioma, small cell lung carcinoma, and melanoma. J. Nucl. Med. *47*, 1599–1606.
7. Kong, G., Grozinsky-Glasberg, S., Hofman, M.S., Callahan, J., Meirovitz, A., Maimon, O., Pattison, D.A., Gross, D.J., and Hicks, R.J. (2017). Efficacy of peptide receptor radionuclide therapy for functional metastatic paraganglioma and pheochromocytoma. J. Clin. Endocrinol. Metab. *102*, 3278–3287.
8. Dingli, D., Peng, K.W., Harvey, M.E., Greipp, P.R., O'Connor, M.K., Cattaneo, R., Morris, J.C., and Russell, S.J. (2004). Image-guided radiovirotherapy for multiple myeloma using a recombinant measles virus expressing the thyroidal sodium iodide symporter. Blood *103*, 1641–1646.
9. Ottolino-Perry KaM, J.A. (2010). Viral introduction of receptors for targeted radiotherapy. In Monoclonal Antibody And Peptide-Targeted Radiotherapy Of Cancer, R.M. Reilly, ed., pp. 349–395.
10. McCart, J.A., Mehta, N., Scollard, D., Reilly, R.M., Carrasquillo, J.A., Tang, N., Deng, H., Miller, M., Xu, H., Libutti, S.K., et al. (2004). Oncolytic vaccinia virus expressing the human somatostatin receptor SSTR2: molecular imaging after systemic delivery using 111In-pentetreotide. Mol. Ther. *10*, 553–561.
11. Rogers, B.E., Zinn, K.R., Lin, C.Y., Chaudhuri, T.R., and Buchsbaum, D.J. (2002). Targeted radiotherapy with [(90)Y]-SMT 487 in mice bearing human nonsmall cell lung tumor xenografts induced to express human somatostatin receptor subtype 2 with an adenoviral vector. Cancer *94* (4 Suppl), 1298–1305.
12. Li, H., Peng, K.W., Dingli, D., Kratzke, R.A., and Russell, S.J. (2010). Oncolytic measles viruses encoding interferon beta and the thyroidal sodium iodide symporter gene for mesothelioma virotherapy. Cancer Gene Ther. *17*, 550–558.
13. Grünwald, G.K., Vetter, A., Klutz, K., Willhauck, M.J., Schwenk, N., Senekowitsch-Schmidtke, R., Schwaiger, M., Zach, C., Wagner, E., Göke, B., et al. (2013). Systemic image-guided liver cancer radiovirotherapy using dendrimer-coated adenovirus encoding the sodium iodide symporter as theranostic gene. J. Nucl. Med. *54*, 1450–1457.
14. Grünwald, G.K., Klutz, K., Willhauck, M.J., Schwenk, N., Senekowitsch-Schmidtke, R., Schwaiger, M., Zach, C., Göke, B., Holm, P.S., and Spitzweg, C. (2013). Sodium iodide symporter (NIS)-mediated radiovirotherapy of hepatocellular cancer using a conditionally replicating adenovirus. Gene Ther. *20*, 625–633.
15. Li, H., Peng, K.W., and Russell, S.J. (2012). Oncolytic measles virus encoding thyroidal sodium iodide symporter for squamous cell cancer of the head and neck radiovirotherapy. Hum. Gene Ther. *23*, 295–301.
16. Opyrchal, M., Allen, C., Iankov, I., Aderca, I., Schroeder, M., Sarkaria, J., and Galanis, E. (2012). Effective radiovirotherapy for malignant gliomas by using oncolytic measles virus strains encoding the sodium iodide symporter (MV-NIS). Hum. Gene Ther. *23*, 419–427.
17. Li, H., Nakashima, H., Decklever, T.D., Nace, R.A., and Russell, S.J. (2013). HSV-NIS, an oncolytic herpes simplex virus type 1 encoding human sodium iodide symporter for preclinical prostate cancer radiovirotherapy. Cancer Gene Ther. *20*, 478–485.
18. Mansfield, D.C., Kyula, J.N., Rosenfelder, N., Chao-Chu, J., Kramer-Marek, G., Khan, A.A., Roulstone, V., McLaughlin, M., Melcher, A.A., Vile, R.G., et al. (2016). Oncolytic vaccinia virus as a vector for therapeutic sodium iodide symporter gene therapy in prostate cancer. Gene Ther. *23*, 357–368.
19. Warner, S.G., Kim, S.-I., Chaurasiya, S., O'Leary, M.P., Lu, J., Sivanandam, V., Woo, Y., Chen, N.G., and Fong, Y. (2019). A novel chimeric poxvirus encoding hNIS is tumor-tropic, imageable, and synergistic with radioiodine to sustain colon cancer regression. Mol. Ther. Oncolytics *13*, 82–92.
20. Ottolino-Perry, K., Diallo, J.S., Lichty, B.D., Bell, J.C., and McCart, J.A. (2010). Intelligent design: combination therapy with oncolytic viruses. Mol. Ther. *18*, 251–263.
21. Buchsbaum, D.J., Rogers, B.E., Khazaeli, M.B., Mayo, M.S., Milenic, D.E., Kashmiri, S.V., Anderson, C.J., Chappell, L.L., Brechbiel, M.W., and Curiel, D.T. (1999). Targeting strategies for cancer radiotherapy. Clin. Cancer Res. *5* (10 Suppl), 3048s–3055s.
22. Barton, K.N., Tyson, D., Stricker, H., Lew, Y.S., Heisey, G., Koul, S., de la Zerda, A., Yin, F.F., Yan, H., Nagaraja, T.N., et al. (2003). GENIS: gene expression of sodium iodide symporter for noninvasive imaging of gene therapy vectors and quantification of gene expression in vivo</em&gt. Mol. Ther. *8*, 508–518.
23. Mitrofanova, E., Unfer, R., Vahanian, N., and Link, C. (2006). Rat sodium iodide symporter allows using lower dose of 131I for cancer therapy. Gene Ther. *13*, 1052–1056.
24. Dingli, D., Diaz, R.M., Bergert, E.R., O'Connor, M.K., Morris, J.C., and Russell, S.J. (2003). Genetically targeted radiotherapy for multiple myeloma. Blood *102*, 489–496.
25. Thorne, S.H., Bartlett, D.L., and Kirn, D.H. (2005). The use of oncolytic vaccinia viruses in the treatment of cancer: a new role for an old ally? Curr. Gene Ther. *5*, 429–443.
26. Guse, K., Cerullo, V., and Hemminki, A. (2011). Oncolytic vaccinia virus for the treatment of cancer. Expert Opin. Biol. Ther. *11*, 595–608.
27. Breitbach, C.J., Arulanandam, R., De Silva, N., Thorne, S.H., Patt, R., Daneshmand, M., Moon, A., Ilkow, C., Burke, J., Hwang, T.H., et al. (2013). Oncolytic vaccinia virus disrupts tumor-associated vasculature in humans. Cancer Res. *73*, 1265–1275.
28. Heo, J., Reid, T., Ruo, L., Breitbach, C.J., Rose, S., Bloomston, M., Cho, M., Lim, H.Y., Chung, H.C., Kim, C.W., et al. (2013). Randomized dose-finding clinical trial of oncolytic immunotherapeutic vaccinia JX-594 in liver cancer. Nat. Med. *19*, 329–336.
29. Kim, M.K., Breitbach, C.J., Moon, A., Heo, J., Lee, Y.K., Cho, M., Lee, J.W., Kim, S.G., Kang, D.H., Bell, J.C., et al. (2013). Oncolytic and immunotherapeutic vaccinia induces antibody-mediated complement-dependent cancer cell lysis in humans. Sci. Transl. Med. *5*, 185ra63.
30. Zeh, H.J., Downs-Canner, S., McCart, J.A., Guo, Z.S., Rao, U.N.M., Ramalingam, L., Thorne, S.H., Jones, H.L., Kalinski, P., Wieckowski, E., et al. (2015). First-in-man study of western reserve strain oncolytic vaccinia virus: safety, systemic spread, and antitumor activity. Mol. Ther. *23*, 202–214.
31. Breitbach, C.J., Thorne, S.H., Bell, J.C., and Kirn, D.H. (2012). Targeted and armed oncolytic poxviruses for cancer: the lead example of JX-594. Curr. Pharm. Biotechnol. *13*, 1768–1772.
32. Downs-Canner, S., Guo, Z.S., Ravindranathan, R., Breitbach, C.J., O'Malley, M.E., Jones, H.L., Moon, A., McCart, J.A., Shuai, Y., Zeh, H.J., and Bartlett, D.L. (2016). Phase 1 study of intravenous oncolytic poxvirus (vvDD) in patients with advanced solid cancers. Mol. Ther. *24*, 1492–1501.
33. Minev, B.R., Lander, E., Feller, J.F., Berman, M., Greenwood, B.M., Minev, I., Santidrian, A.F., Nguyen, D., Draganov, D., Killinc, M.O., et al. (2019). First-in-human study of TK-positive oncolytic vaccinia virus delivered by adipose stromal vascular fraction cells. J. Transl. Med. *17*, 271.
34. Trujillo, M.A., Oneal, M.J., McDonough, S., Qin, R., and Morris, J.C. (2010). A probasin promoter, conditionally replicating adenovirus that expresses the sodium iodide symporter (NIS) for radiovirotherapy of prostate cancer. Gene Ther. *17*, 1325–1332.
35. Carlson, S.K., Classic, K.L., Hadac, E.M., Dingli, D., Bender, C.E., Kemp, B.J., and Russell, S.J. (2009). Quantitative molecular imaging of viral therapy for pancreatic cancer using an engineered measles virus expressing the sodium-iodide symporter reporter gene. AJR. Am. J. Roentgenol. *192*, 279–287.

36. Msaouel, P., Iankov, I.D., Allen, C., Aderca, I., Federspiel, M.J., Tindall, D.J., Morris, J.C., Koutsilieris, M., Russell, S.J., and Galanis, E. (2009). Noninvasive imaging and radiovirotherapy of prostate cancer using an oncolytic measles virus expressing the sodium iodide symporter. Mol. Ther. *17*, 2041–2048.

37. Penheiter, A.R., Wegman, T.R., Classic, K.L., Dingli, D., Bender, C.E., Russell, S.J., and Carlson, S.K. (2010). Sodium iodide symporter (NIS)-mediated radiovirotherapy for pancreatic cancer. AJR. Am. J. Roentgenol. *195*, 341–349.

38. Merron, A., Baril, P., Martin-Duque, P., de la Vieja, A., Tran, L., Briat, A., Harrington, K.J., McNeish, I.A., and Vassaux, G. (2010). Assessment of the Na/I symporter as a reporter gene to visualize oncolytic adenovirus propagation in peritoneal tumours. Eur. J. Nucl. Med. Mol. Imaging *37*, 1377–1385.

39. Hutzen, B., Pierson, C.R., Russell, S.J., Galanis, E., Raffel, C., and Studebaker, A.W. (2012). Treatment of medulloblastoma using an oncolytic measles virus encoding the thyroidal sodium iodide symporter shows enhanced efficacy with radioiodine. BMC Cancer *12*, 508.

40. Hasegawa, K., Pham, L., O'Connor, M.K., Federspiel, M.J., Russell, S.J., and Peng, K.W. (2006). Dual therapy of ovarian cancer using measles viruses expressing carcinoembryonic antigen and sodium iodide symporter. Clin. Cancer Res. *12*, 1868–1875.

41. Goel, A., Carlson, S.K., Classic, K.L., Greiner, S., Naik, S., Power, A.T., Bell, J.C., and Russell, S.J. (2007). Radioiodide imaging and radiovirotherapy of multiple myeloma using VSV(Delta51)-NIS, an attenuated vesicular stomatitis virus encoding the sodium iodide symporter gene. Blood *110*, 2342–2350.

42. Chalikonda, S., Kivlen, M.H., O'Malley, M.E., Eric Dong, X.D., McCart, J.A., Gorry, M.C., Yin, X.Y., Brown, C.K., Zeh, H.J., 3rd, Guo, Z.S., and Bartlett, D.L. (2008). Oncolytic virotherapy for ovarian carcinomatosis using a replication-selective vaccinia virus armed with a yeast cytosine deaminase gene. Cancer Gene Ther. *15*, 115–125.

43. Acuna, S.A., Ottolino-Perry, K., Çako, B., Tang, N., Angarita, F.A., and McCart, J.A. (2014). Oncolytic vaccinia virus as an adjuvant treatment to cytoreductive surgery for malignant peritoneal mesothelioma. Ann. Surg. Oncol. *21*, 2259–2266.

44. Thirunavukarasu, P., Sathaiah, M., Gorry, M.C., O'Malley, M.E., Ravindranathan, R., Austin, F., Thorne, S.H., Guo, Z.S., and Bartlett, D.L. (2013). A rationally designed A34R mutant oncolytic poxvirus: improved efficacy in peritoneal carcinomatosis. Mol. Ther. *21*, 1024–1033.

45. Ottolino-Perry, K., Tang, N., Head, R., Ng, C., Arulanandam, R., Angarita, F.A., Acuna, S.A., Chen, Y., Bell, J., Dacosta, R.S., and McCart, J.A. (2014). Tumor vascularization is critical for oncolytic vaccinia virus treatment of peritoneal carcinomatosis. Int. J. Cancer *134*, 717–730.

46. Ottolino-Perry, K., Acuna, S.A., Angarita, F.A., Sellers, C., Zerhouni, S., Tang, N., and McCart, J.A. (2015). Oncolytic vaccinia virus synergizes with irinotecan in colorectal cancer. Mol. Oncol. *9*, 1539–1552.

47. Chou, T.C., and Talalay, P. (1984). Quantitative analysis of dose-effect relationships: the combined effects of multiple drugs or enzyme inhibitors. Adv. Enzyme Regul. *22*, 27–55.

48. McCart, J.A., Ward, J.M., Lee, J., Hu, Y., Alexander, H.R., Libutti, S.K., Moss, B., and Bartlett, D.L. (2001). Systemic cancer therapy with a tumor-selective vaccinia virus mutant lacking thymidine kinase and vaccinia growth factor genes. Cancer Res. *61*, 8751–8757.

49. Naik, A.M., Chalikonda, S., McCart, J.A., Xu, H., Guo, Z.S., Langham, G., Gardner, D., Mocellin, S., Lokshin, A.E., Moss, B., et al. (2006). Intravenous and isolated limb perfusion delivery of wild type and a tumor-selective replicating mutant vaccinia virus in nonhuman primates. Hum. Gene Ther. *17*, 31–45.

50. Lee, J.H., Roh, M.S., Lee, Y.K., Kim, M.K., Han, J.Y., Park, B.H., Trown, P., Kirn, D.H., and Hwang, T.H. (2010). Oncolytic and immunostimulatory efficacy of a targeted oncolytic poxvirus expressing human GM-CSF following intravenous administration in a rabbit tumor model. Cancer Gene Ther. *17*, 73–79.

51. Lewis, J.S., Wang, M., Laforest, R., Wang, F., Erion, J.L., Bugaj, J.E., Srinivasan, A., and Anderson, C.J. (2001). Toxicity and dosimetry of (177)Lu-DOTA-Y3-octreotate in a rat model. Int. J. Cancer *94*, 873–877.

52. Hennrich, U., and Kopka, K. (2019). Lutathera(®): the first FDA- and EMA-approved radiopharmaceutical for peptide receptor radionuclide therapy. Pharmaceuticals (Basel, Switzerland) *12*, 114.

53. Toth-Fejel, S., and Pommier, R.F. (2004). Relationships among delay of diagnosis, extent of disease, and survival in patients with abdominal carcinoid tumors. Am. J. Surg. *187*, 575–579.

54. Koppe, M.J., Boerman, O.C., Oyen, W.J.G., and Bleichrodt, R.P. (2006). Peritoneal carcinomatosis of colorectal origin: incidence and current treatment strategies. Ann. Surg. *243*, 212–222.

55. Metz, D.C., and Jensen, R.T. (2008). Gastrointestinal neuroendocrine tumors: pancreatic endocrine tumors. Gastroenterology *135*, 1469–1492.

56. Touchefeu, Y., Khan, A.A., Borst, G., Zaidi, S.H., McLaughlin, M., Roulstone, V., Mansfield, D., Kyula, J., Pencavel, T., Karapanagiotou, E.M., et al. (2013). Optimising measles virus-guided radiovirotherapy with external beam radiotherapy and specific checkpoint kinase 1 inhibition. Radiother. Oncol. *108*, 24–31.

57. Dingli, D., Cascino, M.D., Josić, K., Russell, S.J., and Ž, B. (2006). Mathematical modeling of cancer radiovirotherapy. Math. Biosci. *199*, 55–78.

58. Grünwald, G.K., Vetter, A., Klutz, K., Willhauck, M.J., Schwenk, N., Senekowitsch-Schmidtke, R., Schwaiger, M., Zach, C., Wagner, E., Göke, B., et al. (2013). EGFR-targeted adenovirus dendrimer coating for improved systemic delivery of the theranostic NIS gene. Mol. Ther. Nucleic Acids *2*, e131.

59. Trujillo, M.A., Oneal, M.J., McDonough, S.J., and Morris, J.C. (2013). Viral dose, radioiodide uptake, and delayed efflux in adenovirus-mediated NIS radiovirotherapy correlates with treatment efficacy. Gene Ther. *20*, 567–574.

60. Trujillo, M.A., Oneal, M.J., McDonough, S., Qin, R., and Morris, J.C. (2012). A steep radioiodine dose response scalable to humans in sodium-iodide symporter (NIS)-mediated radiovirotherapy for prostate cancer. Cancer Gene Ther. *19*, 839–844.

61. Oneal, M.J., Trujillo, M.A., Davydova, J., McDonough, S., Yamamoto, M., and Morris, J.C. (2013). Effect of increased viral replication and infectivity enhancement on radioiodide uptake and oncolytic activity of adenovirus vectors expressing the sodium iodide symporter. Cancer Gene Ther. *20*, 195–200.

62. Akinlolu, O., Ottolino-Perry, K., McCart, J.A., and Reilly, R.M. (2010). Antiproliferative effects of 111In- or 177Lu-DOTATOC on cells exposed to low multiplicity-of-infection double-deleted vaccinia virus encoding somatostatin subtype-2 receptor. Cancer Biother. Radiopharm. *25*, 325–333.

63. Touchefeu, Y., Franken, P., and Harrington, K.J. (2012). Radiovirotherapy: principles and prospects in oncology. Curr. Pharm. Des. *18*, 3313–3320.

64. Schmitt, A., Bernhardt, P., Nilsson, O., Ahlman, H., Kölby, L., Schmitt, J., and Forssel-Aronsson, E. (2003). Biodistribution and dosimetry of 177Lu-labeled [DOTA0,Tyr3] octreotate in male nude mice with human small cell lung cancer. Cancer Biother. Radiopharm. *18*, 593–599.

65. Kölby, L., Bernhardt, P., Johanson, V., Schmitt, A., Ahlman, H., Forssell-Aronsson, E., Mäcke, H., and Nilsson, O. (2005). Successful receptor-mediated radiation therapy of xenografted human midgut carcinoid tumour. Br. J. Cancer *93*, 1144–1151.

66. Svensson, J., Mölne, J., Forssell-Aronsson, E., Konijnenberg, M., and Bernhardt, P. (2012). Nephrotoxicity profiles and threshold dose values for [177Lu]-DOTATATE in nude mice. Nucl. Med. Biol. *39*, 756–762.

67. Kulkarni, H.R., Schuchardt, C., and Baum, R.P. (2013). Peptide receptor radionuclide therapy with (177)Lu labeled somatostatin analogs DOTATATE and DOTATOC: contrasting renal dosimetry in the same patient. Recent Results Cancer Res. *194*, 551–559.

68. Reubi, J.C., Mäcke, H.R., and Krenning, E.P. (2005). Candidates for peptide receptor radiotherapy today and in the future. J. Nucl. Med. *46* (*Suppl 1*), 67s–75s.

69. Willmon, C., Harrington, K., Kottke, T., Prestwich, R., Melcher, A., and Vile, R. (2009). Cell carriers for oncolytic viruses: fed Ex for cancer therapy. Mol. Ther. *17*, 1667–1676.

70. Smith, E., Breznik, J., and Lichty, B.D. (2011). Strategies to enhance viral penetration of solid tumors. Hum. Gene Ther. *22*, 1053–1060.

71. Guo, Z.S., Parimi, V., O'Malley, M.E., Thirunavukarasu, P., Sathaiah, M., Austin, F., and Bartlett, D.L. (2010). The combination of immunosuppression and carrier cells significantly enhances the efficacy of oncolytic poxvirus in the pre-immunized host. Gene Ther. *17*, 1465–1475.

72. Schäfer, S., Weibel, S., Donat, U., Zhang, Q., Aguilar, R.J., Chen, N.G., and Szalay, A.A. (2012). Vaccinia virus-mediated intra-tumoral expression of matrix metalloproteinase 9 enhances oncolysis of PC-3 xenograft tumors. BMC Cancer *12*, 366.

73. Vegt, E., de Jong, M., Wetzels, J.F.M., Masereeuw, R., Melis, M., Oyen, W.J.G., Gotthardt, M., and Boerman, O.C. (2010). Renal toxicity of radiolabeled peptides and antibody fragments: mechanisms, impact on radionuclide therapy, and strategies for prevention. J. Nucl. Med. *51*, 1049–1058.

74. Gupta, S.K., Singla, S., and Bal, C. (2012). Renal and hematological toxicity in patients of neuroendocrine tumors after peptide receptor radionuclide therapy with 177Lu-DOTATATE. Cancer Biother. Radiopharm. *27*, 593–599.

75. Wallace, W.H.B., Thomson, A.B., and Kelsey, T.W. (2003). The radiosensitivity of the human oocyte. Hum. Reprod. *18*, 117–121.

76. McCart, J.A., Puhlmann, M., Lee, J., Hu, Y., Libutti, S.K., Alexander, H.R., and Bartlett, D.L. (2000). Complex interactions between the replicating oncolytic effect and the enzyme/prodrug effect of vaccinia-mediated tumor regression. Gene Ther. *7*, 1217–1223.

77. Kammar, P.S., Engineer, R., Patil, P.S., Ostwal, V., Shylasree, T.S., and Saklani, A.P. (2017). Ovarian metastases of colorectal origin: treatment patterns and factors affecting outcomes. Indian J. Surg. Oncol. *8*, 519–526.

78. Kunikowska, J., Królicki, L., Hubalewska-Dydejczyk, A., Mikołajczak, R., Sowa-Staszczak, A., and Pawlak, D. (2011). Clinical results of radionuclide therapy of neuroendocrine tumours with 90Y-DOTATATE and tandem 90Y/177Lu-DOTATATE: which is a better therapy option? Eur. J. Nucl. Med. Mol. Imaging *38*, 1788–1797.

79. Kunikowska, J., Królicki, L., Sowa-Staszczak, A., Pawlak, D., Hubalewska-Dydejczyk, A., and Mikołajczak, R. (2013). Nephrotoxicity after PRRT - still a serious clinical problem? Renal toxicity after peptide receptor radionuclide therapy with 90Y-DOTATATE and 90Y/177Lu-DOTATATE. Endokrynol. Pol. *64*, 13–20.

80. Mothersill, C., and Seymour, C.B. (2010). The Bystander Effect in Targeted Radiotherapy.

81. Brady, D., O'Sullivan, J.M., and Prise, K.M. (2013). What is the role of the bystander response in radionuclide therapies? Front. Oncol. *3*, 215.

82. Huang, B., Sikorski, R., Kirn, D.H., and Thorne, S.H. (2011). Synergistic anti-tumor effects between oncolytic vaccinia virus and paclitaxel are mediated by the IFN response and HMGB1. Gene Ther. *18*, 164–172.

83. Vacchelli, E., Vitale, I., Tartour, E., Eggermont, A., Sautès-Fridman, C., Galon, J., Zitvogel, L., Kroemer, G., and Galluzzi, L. (2013). Trial watch: anticancer radioimmunotherapy. Oncoimmunology *2*, e25595.

84. Schmidberger, H., Rave-Fränk, M., Lehmann, J., Schweinfurth, S., Rehring, E., Henckel, K., and Hess, C.F. (1999). The combined effect of interferon beta and radiation on five human tumor cell lines and embryonal lung fibroblasts. Int. J. Radiat. Oncol. Biol. Phys. *43*, 405–412.

85. Wang, Y., Radfar, S., and Khong, H.T. (2010). Activated CD4+ T cells enhance radiation effect through the cooperation of interferon-gamma and TNF-alpha. BMC Cancer *10*, 60.

86. Melcher, A., Parato, K., Rooney, C.M., and Bell, J.C. (2011). Thunder and lightning: immunotherapy and oncolytic viruses collide. Mol. Ther. *19*, 1008–1016.

87. Mansfield, D., Pencavel, T., Kyula, J.N., Zaidi, S., Roulstone, V., Thway, K., Karapanagiotou, L., Khan, A.A., McLaughlin, M., Touchefeu, Y., et al. (2013). Oncolytic Vaccinia virus and radiotherapy in head and neck cancer. Oral Oncol. *49*, 108–118.

88. Kyula, J.N., Khan, A.A., Mansfield, D., Karapanagiotou, E.M., McLaughlin, M., Roulstone, V., Zaidi, S., Pencavel, T., Touchefeu, Y., Seth, R., et al. (2014). Synergistic cytotoxicity of radiation and oncolytic Lister strain vaccinia in V600D/EBRAF mutant melanoma depends on JNK and TNF-α signaling. Oncogene *33*, 1700–1712.

89. Dai, M.H., Liu, S.L., Chen, N.G., Zhang, T.P., You, L., Q Zhang, F., Chou, T.C., Szalay, A.A., Fong, Y., and Zhao, Y.P. (2014). Oncolytic vaccinia virus in combination with radiation shows synergistic antitumor efficacy in pancreatic cancer. Cancer Lett. *344*, 282–290.

90. Earl, P.L., Moss, B., Wyatt, L.S., and Carroll, M.W. (2001). Generation of recombinant vaccinia viruses. Curr. Protoc. Mol. Biol.. Chapter 16:Unit16.17.

91. Wild, D., Schmitt, J.S., Ginj, M., Mäcke, H.R., Bernard, B.F., Krenning, E., De Jong, M., Wenger, S., and Reubi, J.C. (2003). DOTA-NOC, a high-affinity ligand of somatostatin receptor subtypes 2, 3 and 5 for labelling with various radiometals. Eur. J. Nucl. Med. Mol. Imaging *30*, 1338–1347.

92. Baer, A., and Kehn-Hall, K. (2014). Viral concentration determination through plaque assays: using traditional and novel overlay systems. J. Vis. Exp. e52065.